# Affordable Indoor Air Quality Monitoring and Alert System for Particulate Matter ($PM_{1.0}, PM_{2,5}, PM_{10}$)

**Y. Abdullahi[1], I. G. Saidu[2], M. B. Abdullahi[3], and K. A. Dabai[4]**

**[1]Department of Applied Physics, Umaru Ali Shinkafi Polytechnic, Sokoto, Nigeria.**

**[2,3]Department of Physics, Usmanu Danfodiyo University, Sokoto, Nigeria.**

**[4]Department of Electrical Engineering, Usmanu Danfodiyo University, Sokoto, Nigeria.**

**DOI: https://doi.org/10.51584/IJRIAS.2026.110400042**

**Received: 06 March 2026; Accepted: 12 March 2026; Published: 01 May 2026**

## ABSTRACT

This study presents the design and implementation of a low-cost indoor air quality monitoring and alert system capable of detecting particulate matter *($PM_{1.0}, PM_{2,5}, PM_{10}$)*.The system integrates real-time sensing, data acquisition, and an alert mechanism using LED indicators and a buzzer. Experimental results demonstrated strong dynamic responsiveness between particulate matter concentrations, exposure duration, and pollutant density, validating the sensor's sensitivity and measurement stability under controlled indoor conditions. The prototype effectively detected rapid changes in air quality, issued timely alerts under unhealthy conditions, and returned toward baseline values after exposure. These findings highlight its reliability, affordability, and suitability for indoor applications, particularly in resource-limited environments.

**Keywords:** Air Quality Monitoring; Particulate Matter; Indoor Pollution; Low-cost Sensors; Real-time Alerts

## INTRODUCTION

Air pollution remains a critical global challenge, with particulate matter (PM) identified as one of the most harmful pollutants to human health (Mukherjee & Agrawal, 2017). Fine particles such as $PM_{2.5}$ *and* $PM_{10}$ are strongly associated with respiratory and cardiovascular diseases (Zhao et al., 2017). Even more concerning is $PM_{1.0}$ which can penetrate deep into the lungs and potentially enter the bloodstream, posing significant health risks (Johari et al., 2017). Particulate matter originates from both natural and anthropogenic sources. $PM_{10}$ typically arises from mechanical processes such as road dust and construction activities (Thorpe & Harrison, 2008), while $PM_{2.5}$ is largely produced by combustion sources, including vehicle emissions and industrial processes, $PM_{1.0}$ often generated indoors from activities such as smoking, cooking, and incense burning, is particularly hazardous due to its ultrafine size and prolonged suspension time (Huang et al., 2017).

Although conventional air quality monitoring stations provide highly accurate measurements, their high cost and limited spatial coverage restrict access to localized real-time air quality information (Concas et al., 2021). To address these limitations low-cost sensor-based monitoring systems using devices such as the PMS5003 and DHT11 have emerged as practical alternatives (Ji et al., 2010). Prior studies demonstrated that such systems can be effective when calibrated and validated through controlled experiments, for example, simulating indoor pollution with incense burning (Silva et al., 2026).

Despite these advances, major gaps remain, most low-cost systems focus primarily on $PM_{2.5}$ *and* $PM_{10}$ neglecting $PM_{1.0}$ (Silva et al., 2026). Furthermore, many commercial devices are expensive, lack integrated real-time alerts, or do not adequately address indoor air pollution, even though individuals spend up to 90% of their time indoors (Kumar et al., 2016). This gap highlights the need for affordable, reliable, and user-friendly solutions.

ISSN No. 2454-6194 | DOI: 10.51584/IJRIAS |Volume XI Issue IV April 2026

In this work, we present the development of a low-cost, Arduino-based air quality monitoring system that measures $PM_{1.0}$, $PM_{2.5}$, and $PM_{10}$ simultaneously. The system classifies air quality using Air Quality Index (AQI) standards and provides real-time alerts through LED indicators and buzzer alarms. Additionally, live data are displayed on an LCD, and validation is performed through controlled indoor simulations to ensure sensor reliability and alert responsiveness. The proposed system contributes an accessible and practical solution for homes, schools, and public spaces, particularly in regions lacking advanced monitoring technologies.

## RESEARCH METHOD

This research was conducted through a structured methodology, consisting of design, simulation, and experimental validation stages. The study was organized chronologically into the following stages: system design, hardware circuit development, programmed logic implementation, simulation testing, and experimental setup with real-time validation. Each stage is explained in detail below, supported by related references.

### System Design

The project implements a real-time indoor air quality monitoring and alert system based on an Arduino Uno embedded design. The system architecture is divided into three functional layers: sensing, processing, and output/alert, as illustrated in Figure 1.

- Sensing layer: The PMS5003 sensor measures $PM_{1.0}$, $PM_{2.5}$, and $PM_{10}$, while the DHT11 sensor records ambient temperature and humidity.
- Processing layer: An Arduino Uno microcontroller analyzes sensor data and classifies readings into Air Quality Index (AQI) categories using predefined thresholds.
- Output/alert layer: Results are displayed on a 16×2 LCD. Additionally, a piezoelectric buzzer and LED provide real-time audible and visual alerts when PM concentrations exceed safe limits.

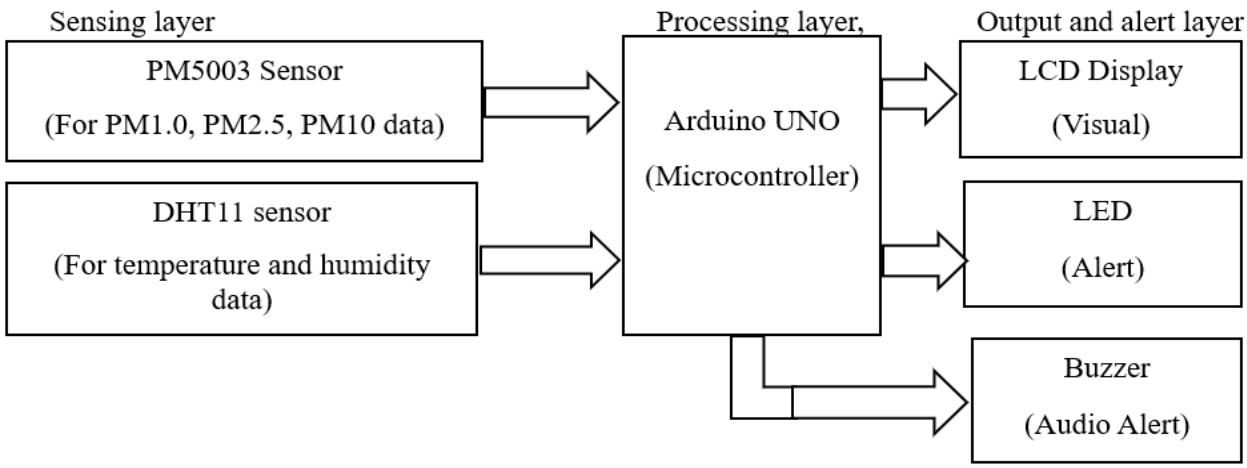


Figure 1. Block diagram of the air quality monitoring system

The Arduino Uno was chosen due to its low cost, ease of programming, and sufficient I/O support (Barbon et al., 2016). The PMS5003 sensor was selected for its reliable UART-based particulate measurement, particularly its ability to capture $PM_{1.0}$, which is often overlooked in low-cost systems (Alfano et al., 2020). The DHT11 sensor complements the system by monitoring environmental conditions (Anuar et al., 2024). An LCD display, buzzer, and LED complete the alert system, ensuring user-friendly output.

### Hardware Circuit Design

The hardware integration is shown in Figure 2, with pin mappings described as follows:

- PMS5003 → TX: D10, RX: D11, powered by 5V/GND.

ISSN No. 2454-6194 | DOI: 10.51584/IJRIAS |Volume XI Issue IV April 2026

- DHT11 → Data: D2, powered by 5V/GND.
- LCD (16×2, 4-bit mode) → RS: D12, E: D9, D4–D7: pins 5, 4, 3, 6.
- Buzzer → positive: D8, negative: GND.
- LED → anode: D7 (through 220Ω resistor), cathode: GND.

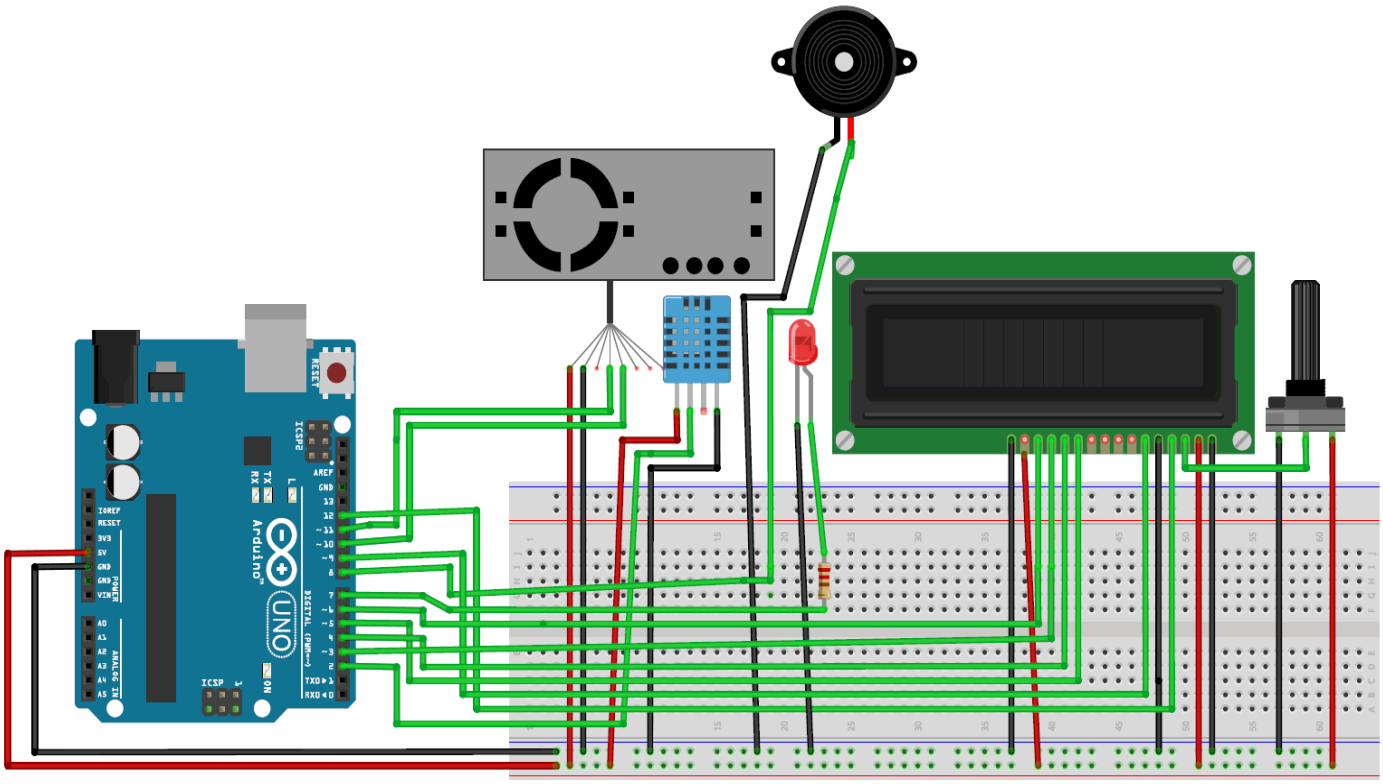

Figure 2. Hardware circuit design

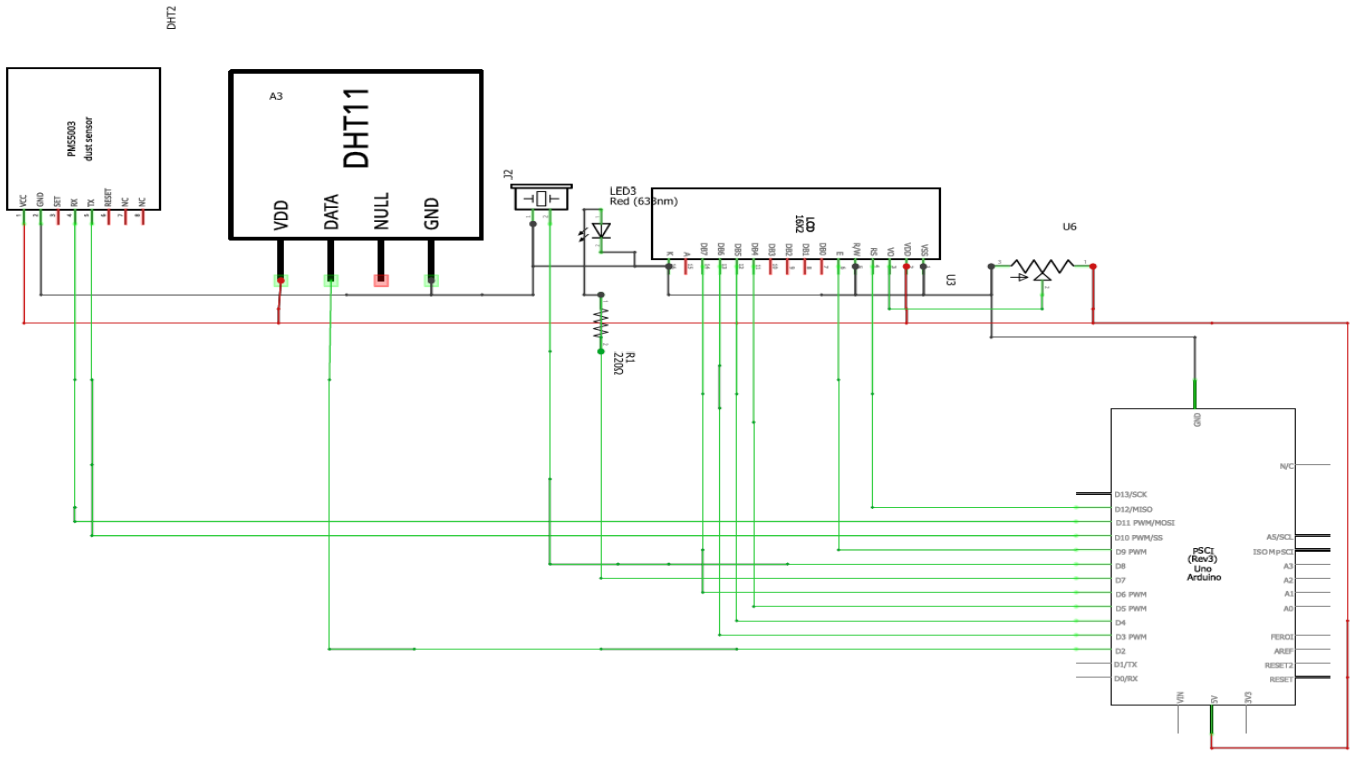


Figure 3. Schematic of hardware circuit connections

ISSN No. 2454-6194 | DOI: 10.51584/IJRIAS |Volume XI Issue IV April 2026

This modular configuration allowed flexible prototyping using jumper wires and a breadboard, with power supplied via USB or battery pack.

**Mathematical Logic and AQI Classification**

The AQI classification follows U.S. EPA breakpoints, $PM_{2.5}$, $PM_{10}$, and a custom $PM_{1.0}$ scale were used, as shown in Equations (1)– (3) (Elabd et al., 2026). For general AQI computation, Equation (4) was applied.

$$\text{Category}_{PM2.5}(x) = \begin{cases} \text{Good} \rightarrow x \leq 12.0 \\ \text{Moderate} \rightarrow 12.0 < x \leq 35.4 \\ \text{Unhealthy for Sensitive Groups} \rightarrow 35.4 < x \leq 55.4 \\ \text{Unhealthy} \rightarrow 55.4 < x \leq 150.4 \\ \text{Very Unhealthy} \rightarrow 150.4 < x \leq 250.4 \\ \text{Hazardous} \rightarrow x > 250.4 \end{cases} \quad (1)$$

$$Category_{PM1.0}(x) = \begin{cases} \text{Good} \rightarrow x \leq 8.0 \\ \text{Moderate} \rightarrow 8.0 < x \leq 25.0 \\ \text{Unhealthy for Sensitive Groups} \rightarrow 25.0 < x \leq 40.0 \\ \text{Unhealthy} \rightarrow 40.0 < x \leq 100.0 \\ \text{Very Unhealthy} \rightarrow 100.0 < x \leq 170.0 \\ \text{Hazardous} \rightarrow x > 170.0 \end{cases} \quad (2)$$

$$Category_{PM10}(x) = \begin{cases} \text{Good} \rightarrow x \leq 54.0 \\ \text{Moderate} \rightarrow 54.0 < x \leq 154.0 \\ \text{Unhealthy for Sensitive Groups} \rightarrow 154.0 < x \leq 254.0 \\ \text{Unhealthy} \rightarrow 254.0 < x \leq 354.0 \\ \text{"Very Unhealthy} \rightarrow 354.0 < x \leq 424 \\ \text{"Hazardous} \rightarrow x > 424.0 \end{cases} \quad (3)$$

$$\text{AQI} = \left(\frac{I_{high} - I_{low}}{C_{high} - C_{low}}\right) \times (C - C_{low}) + I_{low} \quad (4)$$

Were:

- $C$ = measured pollutant concentration
- $C_{high}$ , $C_{low}$ = *concentrations breakpoints*
- $I_{high}$ , $I_{low}$ = AQI breakpoints

**Simulation**

Proteus software was used to simulate the hardware and logic before implementation. The complete simulation setup is shown in figure 4. The Arduino sketch (Figure 5) was compiled into a hex file (Figure 6) and uploaded into the virtual Arduino for real-time hardware-in-the-loop testing (Figure 7). The simulation results figure 8 confirmed proper sensor readings, AQI categorization, and accurate buzzer/LED responses under hazardous PM concentrations.

ISSN No. 2454-6194 | DOI: 10.51584/IJRIAS |Volume XI Issue IV April 2026

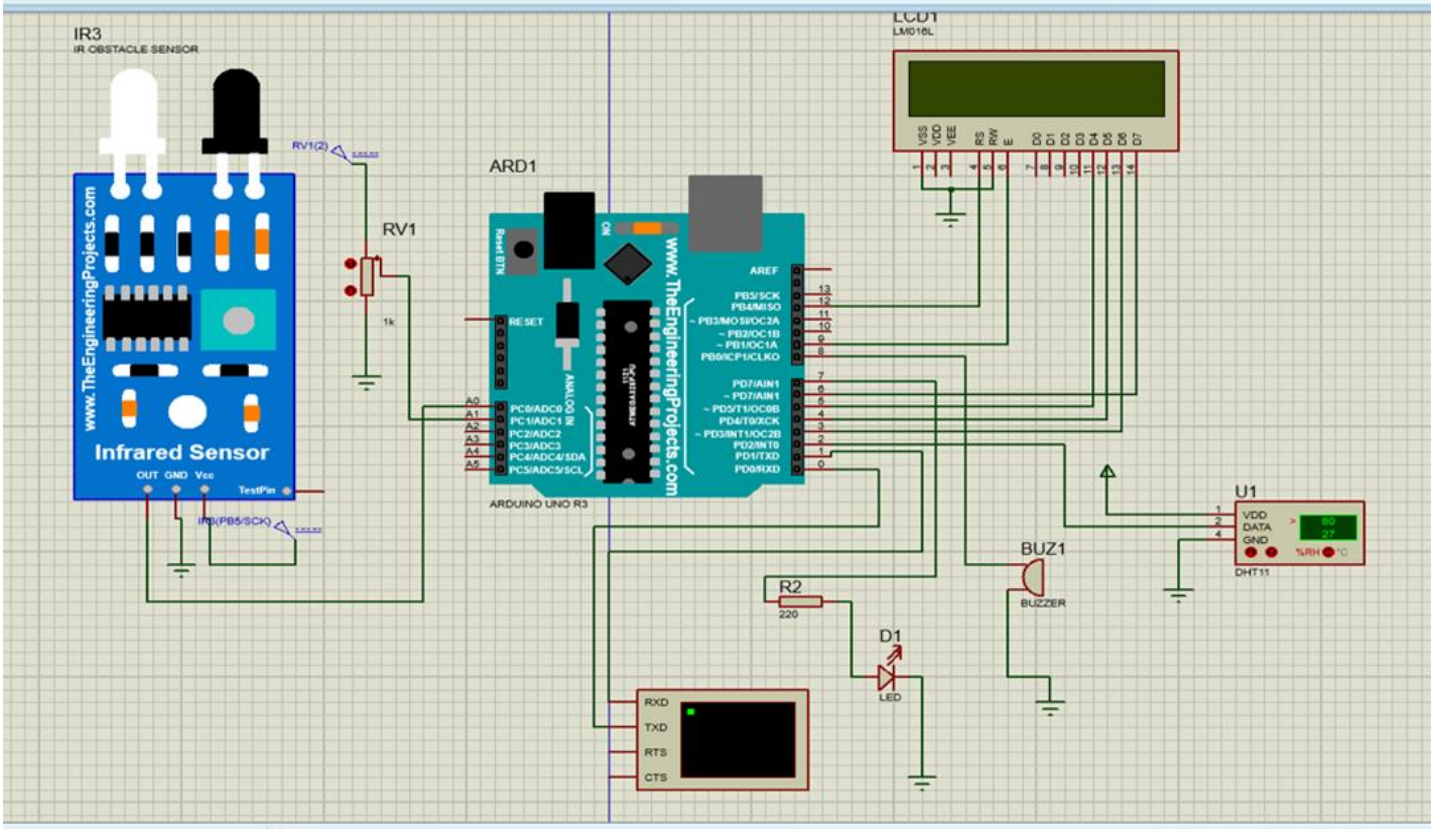


Figure 4. Complete simulation circuit

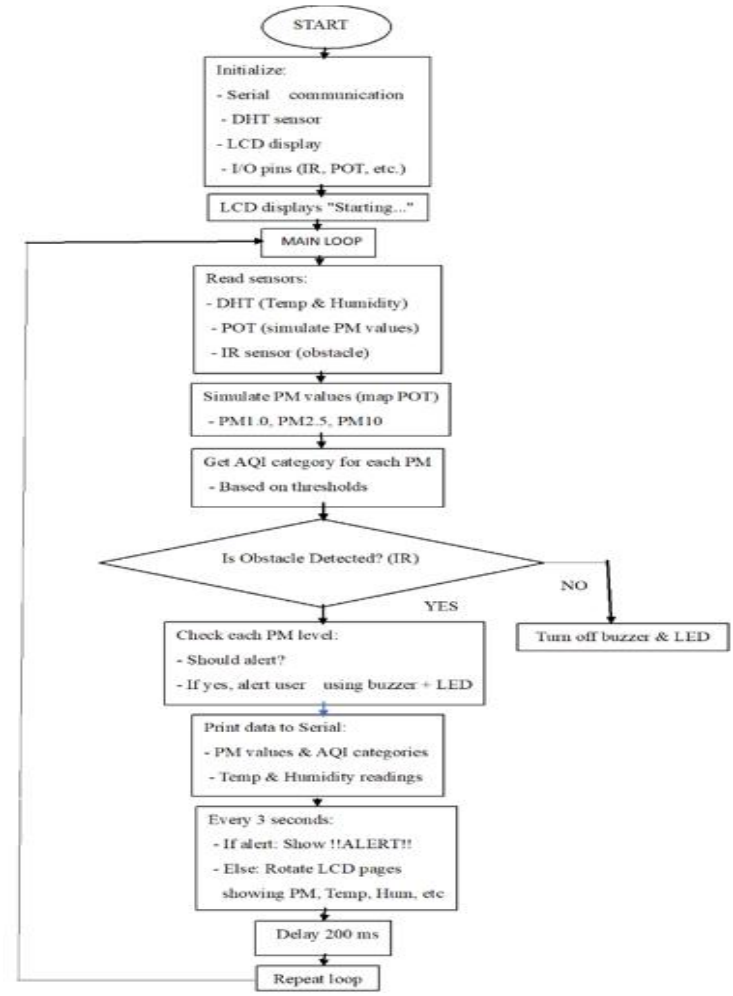


Figure 5. Logic flowchart in simulation

ISSN No. 2454-6194 | DOI: 10.51584/IJRIAS |Volume XI Issue IV April 2026

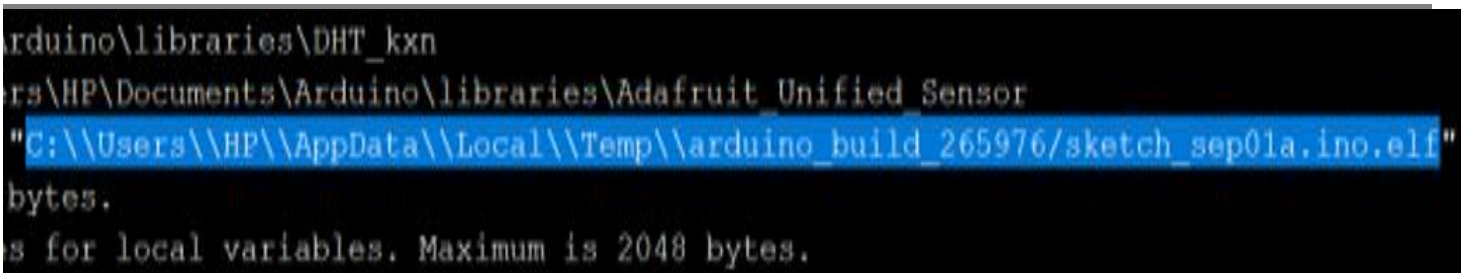


Figure 6. Generated hex file in Arduino IDE

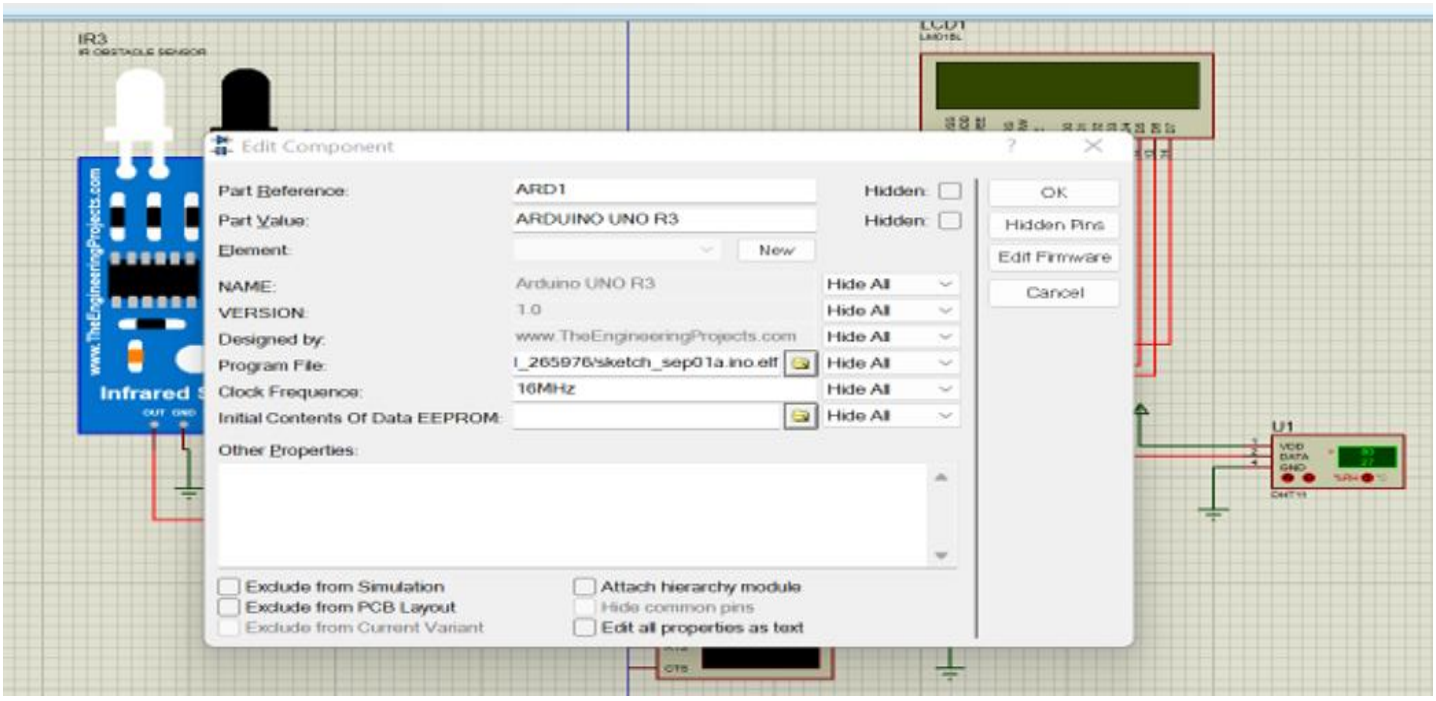


Figure 7. Hex file linked in Proteus simulation

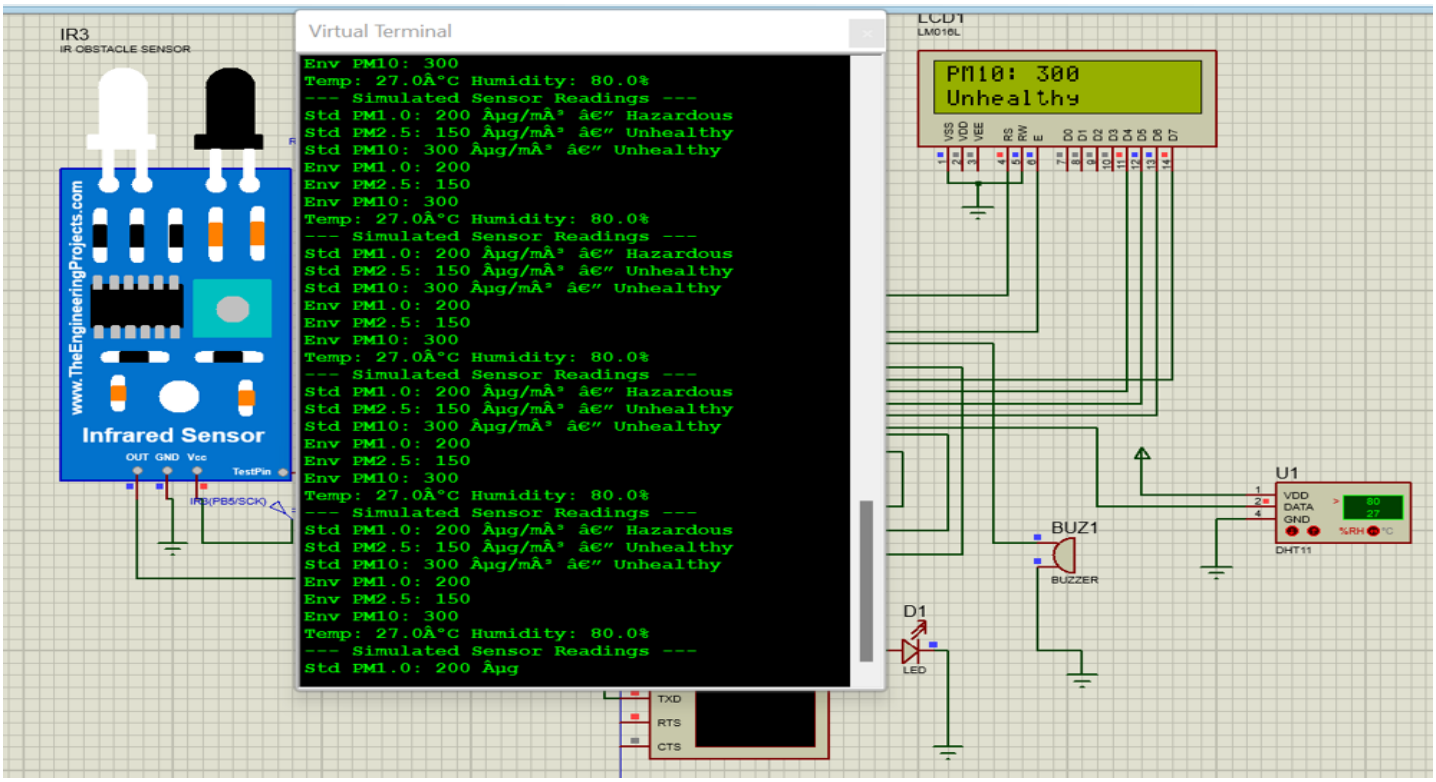


Figure 8. Simulation results

ISSN No. 2454-6194 | DOI: 10.51584/IJRIAS |Volume XI Issue IV April 2026

**Calibration of PMS5003 Sensor Against 9-in-1 Air Quality Detector**

Both the PMS5003 particulate matter sensor and the 9-in-1 Air Quality Detector were co-located within the same sealed indoor environment. To minimize environmental variability, all doors and windows were kept closed, no active pollution sources were present, and airflow disturbances were eliminated. Relative humidity remained reasonably stable throughout the measurement period. Both instruments were allowed to operate continuously for 30 minutes to achieve thermal equilibrium and measurement stability. Following this stabilization period, averaged particulate matter concentrations for $PM_{1.0}, PM_{2.5}$ *and* $PM_{10}$ were recorded from both devices, as shown in Figures 9 and 10. This dataset represents the clean-air baseline condition, under which systematic sensor bias is most clearly observable.

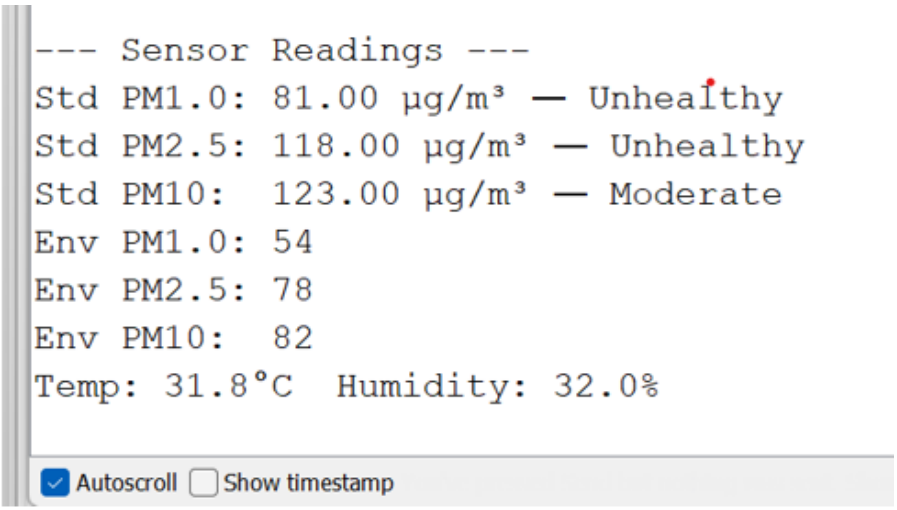


Figure 9. PMS5003 sensor readings under clean-air conditions


Figure 10. 9-in-1 air quality detector readings under clean-air conditions

As shown in Figures 9 and 10, under stable clean-air conditions the PMS5003 consistently reported higher particulate matter concentrations compared with the 9-in-1 Air Quality Detector. Importantly, the magnitude of this discrepancy increased proportionally with concentration rather than remaining constant across particle size fractions. This proportional scaling behavior indicates that the dominant error mechanism is a systematic gain (scaling) error, rather than a fixed baseline offset. Similar proportional bias behaviors have been widely reported in previous evaluations of low-cost optical particulate sensors. Studies have shown that sensors based on light-

ISSN No. 2454-6194 | DOI: 10.51584/IJRIAS |Volume XI Issue IV April 2026

scattering techniques often exhibit concentration-dependent scaling deviations due to particle size distribution sensitivity and internal mass-conversion assumptions (Kloppenborg et al., 2026). Because the 9-in-1 detector did not indicate near-zero particulate levels and a true zero-air chamber was unavailable, baseline offset could not be reliably estimated. Consequently, offset correction was intentionally excluded to avoid over-compensation at low but non-zero concentrations. Consistent with established calibration methodologies for optical PM sensors. baseline offset error was therefore considered negligible relative to gain error (Maag et al., 2018).

**Gain Correction Coefficient Derivation**

Systematic gain error was identified as the dominant source of bias in the PMS5003 measurements based on the proportional discrepancies observed relative to the 9-in-1 Air Quality Detector (Ma et al., 2025) . Gain correction coefficients were derived using a linear scaling model with a zero intercept (Flohr et al., 2018):

$$K = \frac{PM_{reference}}{PM_{raw}} \quad 5$$

Where $PM_{reference}$ is the particulate concentration measured by the 9-in-1 air quality monitor and $PM_{raw}$ is the corresponding PMS5003 sensor output.

Table 1 presents the PMS5003 measurements prior to calibration. The raw PMS5003 values represent the sensor's uncorrected readings, while the reference values correspond to measurements obtained from the 9-in-1 air quality monitor. The Gain (k) represents the calibration factor derived to correct systematic deviations and align the PMS5003 measurements with the reference instrument, all values are reported in their respective units. The observed gain coefficients (< 1.0) confirm that the PMS5003 exhibits systematic overestimation, consistent with prior studies of the Plantower PMS series sensors (Sayahi et al., 2019). Such overestimation is commonly attributed to: Optical scattering sensitivity, particle refractive index dependence and internal mass-conversion assumptions (Benko et al., 2009)

Table 1: calculated gain coefficients k for each particle size channel

| Chennel | Raw PMS5003($\mu g/m^3$) | Reference($\mu g/m^3$) | Gain (K) |
|---|---|---|---|
| PM1.0 | 81 | 39 | 0.48 |
| PM2,5 | 118 | 60 | 0.51 |
| PM10 | 123 | 69 | 0.56 |

Equation (6) applies the gain correction to the raw sensor measurements, this gain-based calibration compensates for the systematic overestimation inherent in the PMS5003's optical mass-conversion process, improves agreement with the reference instrument under clean-air conditions, and establishes a robust baseline for subsequent two-point calibration using incense-generated pollution data.

$$PM_{calibrate} = K \times PM_{raw} \quad (6)$$

Previous studies have demonstrated that gain-only correction models provide stable improvements for optical PM sensors under controlled indoor environments (Zuo, Lai & Iyer, 2023). The logic flowchart for the calibration implementation is shown in Figure 11.

**System Logic and Calibration Implementation**

The flowchart figure 12 illustrates the operational logic of the developed PMS5003 based air quality monitoring system, integrating real-time sensing, calibration, and display functions. Upon startup, the system initializes all hardware components and sensor interfaces, including the PMS5003 particulate sensor, DHT temperature humidity sensor, LCD module, and serial communication. During this initialization stage, calibration parameters specifically gain correction coefficients are loaded into the system. In the setup phase, the serial interface, DHT sensor, and LCD are initialized, and a confirmation message ("PMS Calibrated") is displayed to indicate successful system readiness. The main program loop begins by acquiring ambient temperature and humidity data, followed by continuous checking for the availability of PMS5003 particulate matter data. When valid

ISSN No. 2454-6194 | DOI: 10.51584/IJRIAS |Volume XI Issue IV April 2026

PMS5003 data are detected, the system processes the raw $PM_{1.0}$, $PM_{2.5}$, and $PM_{10}$ measurements. Equation (5), derived from clean-air reference measurements using a 9-in-1 air quality monitor, defines the gain correction coefficients. These coefficients are applied in real time to the PMS5003 outputs using Equation (6), ensuring that systematic gain errors inherent in the sensor's optical mass conversion process are corrected. An offset term is intentionally excluded, consistent with the calibration analysis, to preserve a clean and physically meaningful baseline. The calibrated particulate data, along with temperature and humidity readings, are then displayed on the LCD in a cyclic, multi-page format: $PM_{2.5}$ with AQI, $PM_{1.0}$ and $PM_{10}$, and environmental parameters. The loop executes continuously, enabling uninterrupted environmental monitoring. Overall, this flowchart represents a gain-corrected, offset-free calibration framework that establishes a stable clean-air baseline. This design ensures reliable sensor performance under low-pollution conditions and provides a robust foundation for subsequent two-point calibration using incense-generated particulate matter, as planned in validation procedure.

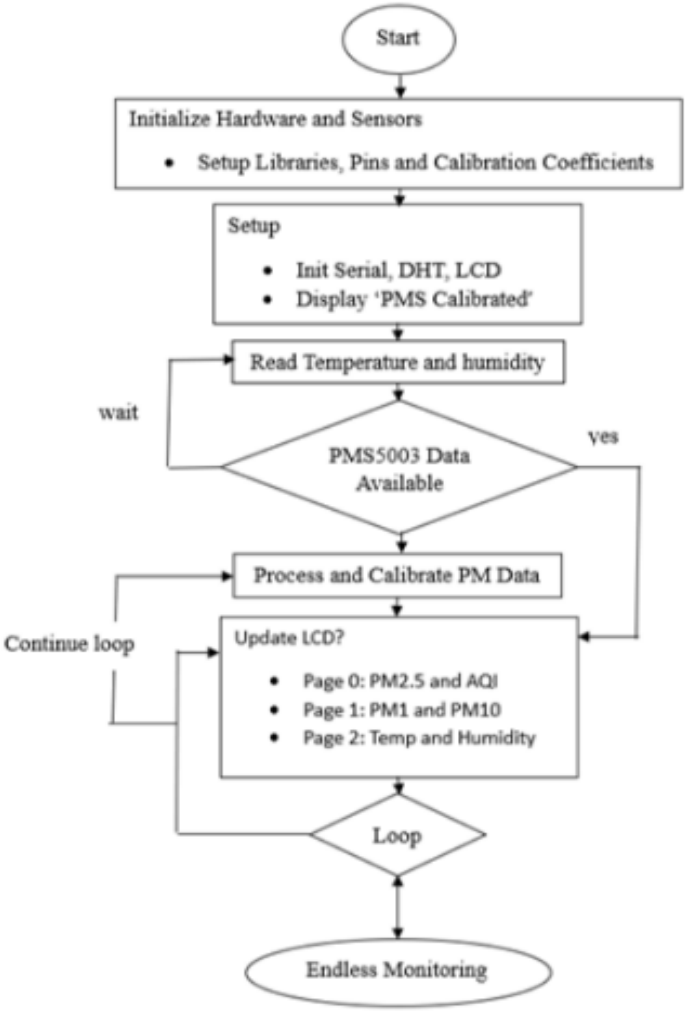


Figure 11. Logic flowchart – PMS5003 gain-calibrated air quality system

**Generation of Pollution Dataset Using Incense**

To generate a controlled high-concentration particulate matter dataset extending beyond clean-air conditions, a pollution experiment was conducted to support two-point (affine) calibration of the PMS5003 sensor against a reference instrument. The PMS5003 sensor and the 9-in-1 air quality detector were positioned side by side, with their sampling inlets separated by approximately 5 cm. Both sensors were placed at the same height and oriented similarly to minimize airflow disturbances and gravitational bias. This configuration ensured that both instruments sampled the same air volume throughout the experiment. To minimize environmental variability: All doors and windows were closed to reduce external air exchange, fans, air conditioners, and other airflow sources were switched off. The room was allowed to stabilize for 15 minutes prior to incense ignition. Temperature and relative humidity were monitored using the DHT11 sensor integrated with the PMS5003 system and the readings displayed by the reference instrument. Before introducing incense, a clean-air baseline

ISSN No. 2454-6194 | DOI: 10.51584/IJRIAS |Volume XI Issue IV April 2026

dataset was recorded. The PMS5003 sensor readings under baseline conditions are presented in Figure 12, while the corresponding measurements from the 9-in-1 reference monitor are shown in Figure 13.

```
--- PMS5003 Gain-Calibrated Output -
PM1.0  Raw: 24.00  Cal: 55.20
PM2.5  Raw: 36.00  Cal: 86.40
PM10   Raw: 37.00  Cal: 98.05
Temp: 30.2 C  RH: 25.0 %
```

Figure 12: PMS5003 sensor results before introducing incense


Figure 13: 9-in-1 air quality detector results before introducing incense

This baseline acquisition step verified that: PMS5003 readings were stable and consistent with previously gain-calibrated clean-air values, reference instrument readings exhibited steady behavior and environmental conditions remained reasonably constant. The baseline segment therefore served as the transition point between clean-air and polluted conditions.

**Measurement Agreement Analysis**

Comparison of the baseline measurements from Figure 13 and Figure 14 demonstrates strong agreement between the gain-calibrated PMS5003 and the reference 9-in-1 air quality detector shown in table 2. The small residual differences observed are consistent with expected sensor tolerances and short-term fluctuations, indicating that the gain-based calibration effectively compensates for systematic bias in the PMS5003 measurements. A larger deviation is observed in relative humidity between Figure 13 and Figure 14: PMS5003, (DHT11): 25 %, 9-in-1 air quality detector: 33 %. This discrepancy is attributable to: The inherent accuracy limitation of the DHT11 sensor (±5 % RH), minor spatial humidity gradients within the indoor environment and differences in sensing technology between the two instruments. Importantly, this variation does not materially affect particulate matter calibration, as PM measurements rely on independent optical detection mechanisms. The baseline measurements presented in Figure 13 and Figure 14 confirm that: Gain-calibrated PMS5003 readings closely align with the reference instrument, systematic overestimation has been substantially reduced, environmental conditions were

ISSN No. 2454-6194 | DOI: 10.51584/IJRIAS |Volume XI Issue IV April 2026

adequately controlled and the experimental setup is suitable for subsequent incense generated pollution analysis. The small residual deviations fall within expected tolerance ranges for low-cost PM sensors (Zheng et al., 2018).

Table 2. Comparison of the baseline measurements from Figure 12 and Figure 13

| Parameter | PMS5003(Figure13) | Reference (Figure 14) | Observation |
|---|---|---|---|
| PM1.0 | 55.20$\mu g/m^3$ | 53$\mu g/m^3$ | Very close agreement |
| PM2.5 | 86.40$\mu g/m^3$ | 82$\mu g/m^3$ | Minor positive deviation |
| PM10 | 98.05$\mu g/m^3$ | 94$\mu g/m^3$ | Minor positive deviation |
| Temperature | 30.2°C | 30°C | Excellent agreement |

**Incense Introduction – Controlled Concentration Increase Phase**

A controlled particulate pollution environment was generated using a single incense stick. The incense was ignited and allowed to burn steadily, positioned approximately 1 meter from both instruments to prevent direct plume impingement. Particulate concentrations increased gradually through natural diffusion, thereby simulating a realistic indoor pollution scenario. Measurements from the PMS5003 sensor were compared with readings obtained from the 9-in-1 Air Quality Detector, which served as a comparative consumer-grade instrument. Measurements were recorded at 1-minute intervals, and the resulting dataset is presented in Table 3.

Table 3: Comparison of PMS5003 and 9-in-1 Air Quality Detector Controlled Concentration Increase Phase (1-Minute Interval)

| Time (min) | Measurement Type | PM1.0 (µg/m³) | PM2.5 (µg/m³) | PM10 (µg/m³) |
|---|---|---|---|---|
| 0 (Baseline) | PM5003Raw | 24.00 | 36.00 | 37.00 |
| | PM5003 Calibrated | 55.20 | 86.40 | 98.05 |
| | 9-in-1 Air Quality | 53.00 | 82.00 | 94.00 |
| 1 | PM5003Raw | 69.00 | 104.00 | 106/00 |
| | PM5003 Calibrated | 158.70 | 249.60 | 249.60 |
| | 9-in-1 Air Quality | 53.00 | 82.00 | 98.00 |
| 2 | PM5003Raw | 84.00 | 136.00 | 141.00 |
| | PM5003 Calibrated | 193.20 | 326.40 | 373.65 |
| | 9-in-1 Air Quality | 53.00 | 82.00 | 94.00 |
| 3 | PM5003Raw | 101.00 | 155.00 | 162.00 |
| | PM5003 Calibrated | 232.30 | 372.00 | 429.30 |
| | 9-in-1 Air Quality | 53.00 | 82.00 | 94.00 |
| 4 | PM5003Raw | 105.00 | 169.00 | 176.00 |
| | PM5003 Calibrated | 241.50 | 405 | 466.40 |
| | Reference Monitor | 53.00 | 82.00 | 94.00 |
| 5 | PM5003Raw | 112.00 | 173.00 | 182.00 |
| | PM5003 Calibrated | 257.60 | 415.00 | 482.30 |
| | 9-in-1 Air Quality | 53.00 | 82.00 | 94.00 |

**Analysis of Concentration Increase Dataset (Table 3)**

Table 3 shown the PMS5003 raw measurements exhibit a clear monotonic increase following incense ignition: $PM_{1.0}$ increased from 24 → 112 µg/m³, $PM_{2.5}$ increased from 36 → 173 µg/m³ and $PM_{10}$ increased from 37 → 182 µg/m³. This trend confirms the sensor's responsiveness to rising particulate concentrations. After gain calibration, the corrected measurements preserved the same temporal pattern, indicating that the calibration process maintains sensor linearity and dynamic behaviors. In contrast, the 9-in-1 detector readings shown in Table 3 remain relatively stable throughout the concentration increase phase. This behavior is consistent with consumer-grade monitoring devices that employ: Internal averaging algorithms, temporal smoothing filters and display stabilization mechanisms such processing reduces short-term variability. Validation during this phase focuses on trend consistency and dynamic response agreement: Although absolute magnitudes differ.

ISSN No. 2454-6194 | DOI: 10.51584/IJRIAS |Volume XI Issue IV April 2026

Table 3 demonstrates that: No contradictory measurements are observed, no inverse trends occur and sensor readings evolve smoothly. The PMS5003 detects concentration rise, while the 9-in-1 detector provides stabilized values. This confirms qualitative validation of sensor response. The data in Table 3 indicate that the PMS5003 exhibits: high temporal sensitivity, rapid response to particulate generation and clear transient tracking. Similar transient tracking capability has been reported in dynamic response evaluations of optical PM sensors (He, Kuerbanjiang, & Dhaniyala, 2020). Whereas the 9-in-1 detector exhibits reduced short-term responsiveness due to internal filtering, this divergence reflects instrument response characteristics, not measurement failure. The relatively stable readings of the 9-in-1 detector are consistent with temporal smoothing behaviors typical of consumer-grade monitors (Singer & Delp, 2018).

**Controlled Concentration Decay Phase Monitoring**

Following the controlled particulate generation phase, the incense source was removed, allowing particulate concentrations within the room to decay naturally. Measurements were recorded at 2-minute intervals, and the resulting dataset is presented in Table 4.

Table 4: Comparison of PMS5003 and 9-in-1 Air Quality Detector, Controlled Concentration Decay Phase Monitoring (2-Minute Interval)

| Time (min) | Measurement Type | PM1.0 (µg/m³) | PM2.5 (µg/m³) | PM10 (µg/m³) |
|---|---|---|---|---|
| **0** | PM5003Raw | 103.00 | 157.00 | 163.00 |
| | PM5003 Calibrated | 236.90 | 376.80 | 376.80 |
| | 9-in-1 Air Quality | 53.00 | 82.00 | 94.00 |
| 2 | PM5003Raw | 99.00 | 148.00 | 155.00 |
| | PM5003 Calibrated | 227.70 | 355.20 | 410.75 |
| | 9-in-1 Air Quality | 53.00 | 82.00 | 94.00 |
| 4 | PM5003Raw | 64.00 | 97.00 | 99.00 |
| | PM5003 Calibrated | 147.20 | 232.80 | 262.35 |
| | Reference Monitor | 53.00 | 82.00 | 94.00 |
| 8 | PM5003Raw | 50.00 | 71.00 | 73.00 |
| | PM5003 Calibrated | 115.00 | 170.00 | 193.00 |
| | 9-in-1 Air Quality | 53.00 | 82.00 | 94.00 |
| 10 | PM5003Raw | 35.00 | 51.00 | 55.00 |
| | PM5003 Calibrated | 80.50 | 122.40 | 145.75 |
| | 9-in-1 Air Quality | 53.00 | 82.00 | 94.00 |
| 12 | PM5003Raw | 22.00 | 32.00 | 34.00 |
| | PM5003 Calibrated | 50.00 | 76.80 | 90.00 |
| | 9-in-1 Air Quality | 53.00 | 82.00 | 94.00 |

**Analysis of Concentration Decay Dataset (Table 4)**

Table 4 shown the PMS5003 raw measurements exhibit a clear monotonic decrease across all particulate size fractions: $PM_{1.0}$ : 103 → 22 µg/m³, $PM_{2.5}$ : 157 → 32 µg/m³ and $PM_{10}$ : 163 → 34 µg/m³, this decay behaviors is physically consistent with expected aerosol dynamics following pollutant removal (Dewage, 2024). The observed reduction can be attributed to: Gravitational settling of suspended particle, diffusive dispersion within the room and natural dilution mechanisms. The smooth decay profile confirms that the PMS5003 sensor effectively tracks decreasing particulate concentrations, the gain-calibrated PMS5003 measurements preserve the same decay trend observed in the raw dataset, this confirms that the gain correction process: Maintains temporal sensor dynamics, does not introduce instability and does not distort decay behaviors. The proportional scaling observed across all measurement intervals further indicates calibration robustness under transient conditions.

In contrast, the readings obtained from the 9-in-1 Air Quality Detector remain relatively stable throughout the decay phase: $PM_{1.0}$ ≈ 53 µg/m³, $PM_{2.5}$ ≈ 82 µg/m³ and $PM_{10}$ ≈ 94 µg/m³. This stability is consistent with the

ISSN No. 2454-6194 | DOI: 10.51584/IJRIAS |Volume XI Issue IV April 2026

operational characteristics of consumer-grade multi-parameter monitors, which commonly employ: Internal averaging algorithms, temporal smoothing filters and display stabilization mechanisms (Perez, 2025). Such filtering suppresses short-term fluctuations and transient variations. Validation during the decay phase provides strong evidence of PMS5003 sensor reliability. The PMS5003 measurements demonstrate: Monotonic reduction, physically realistic decay behavior and absence of oscillatory artefacts, this confirms that the sensor accurately captures pollutant dissipation dynamics. The decay dataset highlights a key performance characteristic of the PMS5003 sensor: Sensitivity to transient environmental changes, reliable tracking of concentration relaxation and stable measurement evolution. This behavior is essential for real-time indoor air quality monitoring applications. Across the entire decay interval: No measurement drift observed, no noise amplification and stable calibrated response. This confirms sensor repeatability and operational stability. At 12 minutes, the PMS5003 calibrated measurements approach: $PM_{1.0} \rightarrow 50.00$ µg/m³, $PM_{2.5} \rightarrow 76.80$ µg/m³ and $PM_{10} \rightarrow 90.00$ µg/m³. These values converge toward the stabilized readings of the 9-in-1 detector, indicating: Natural return toward baseline conditions, absence of sensor drift and physically consistent decay termination. The measurements presented in Table 4 validate that the PMS5003 sensor: Accurately tracks decreasing particulate concentrations, maintains stable calibrated response and exhibits physically consistent decay behavior. Therefore, the PMS5003 sensor is experimentally validated for dynamic indoor particulate monitoring applications. These findings are consistent with previous evaluations of low-cost optical PM sensors, which emphasize strong dynamic response but concentration-dependent scaling bias (Mahajan & Helbing, 2025). The results obtained in this study align with established literature shown in table 5:

Table 5: Established literature

| **Observed Behavior** | **Agreement with prior studies** |
|---|---|
| Systematic gain bias | Widely reported (Sousan et al., 2016) |
| Overestimation tendency | Documented (Sayahi et al., 2019) |
| Strong transient sensitivity | Confirmed (Zheng et al., 2018) |
| Stable gain correction | Supported (Kelly et al., 2017) |

**Experimental Setup**

The physical prototype was assembled on a breadboard (Figure 14) and tested in a controlled environment (Figure 15). A transparent plastic container was used to simulate indoor conditions, with incense sticks providing controlled PM sources.

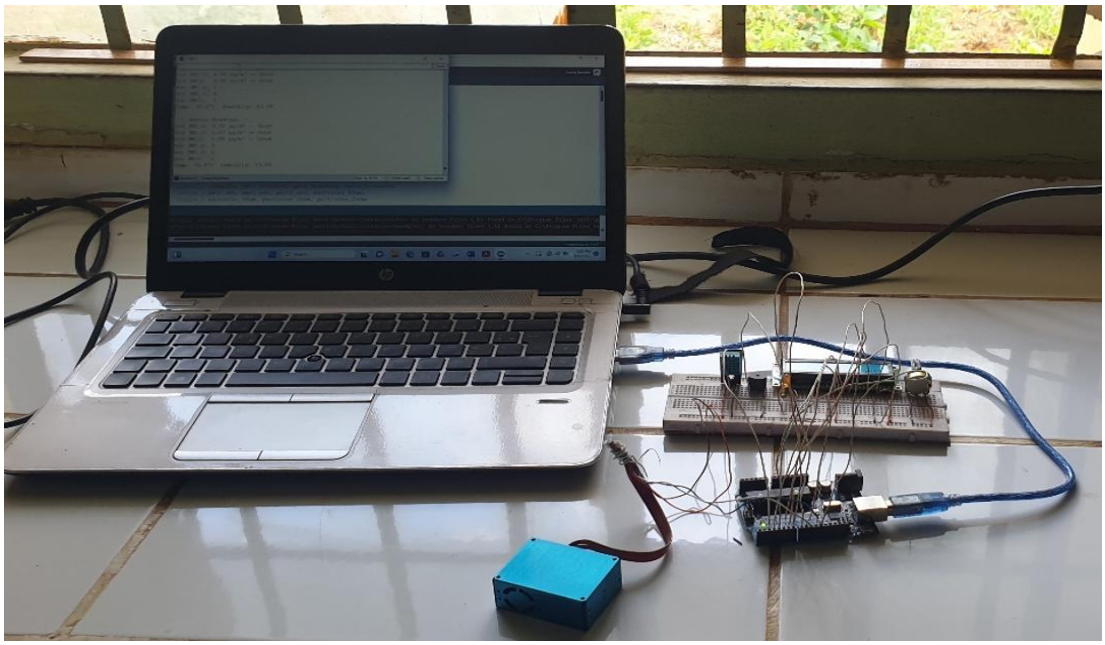

Figure 14. Assembled circuit prototype

ISSN No. 2454-6194 | DOI: 10.51584/IJRIAS |Volume XI Issue IV April 2026

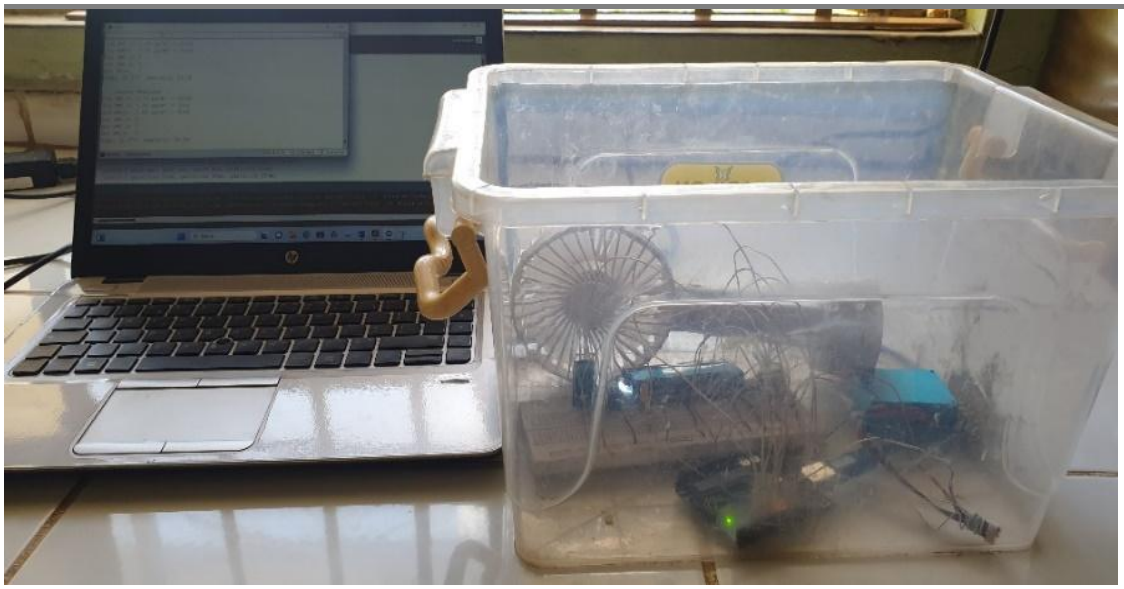

Figure 15. Experimental test setup

**Test Procedure and Data Acquisition**

Controlled tests were conducted using incense sticks:

- Baseline test: System stabilized in clean air (Figure 16),
- Single-stick test: Short 2s exposure increased $PM_{1.0}$, $PM_{2.5}$ and $PM_{10}$ significantly (Figure 17)
- Multiple-stick test: Progressive exposure (2–5 sticks) increased PM levels, logged in Table 6.

Table 6: Logged PM data under multiple incense exposures

| No of sticks | Time(s) | PM1.0 $(ug/m^3)$ | PM2.5$(ug/m^3)$ | PM10$(ug/m^3)$ | Notes |
|---|---|---|---|---|---|
| 0 | 0 | 1 | 4 | 4 | Baseline |
| 1 | 2 | 27 | 40 | 41 | Smoke rising |
| 2 | 4 | 59 | 74 | 76 | Smoke rising |
| 3 | 6 | 126 | 175 | 180 | Smoke rising |
| 4 | 8 | 314 | 578 | 616 | Smoke rising |
| 5 | 10 | 476 | 862 | 876 | Heavy smoke |

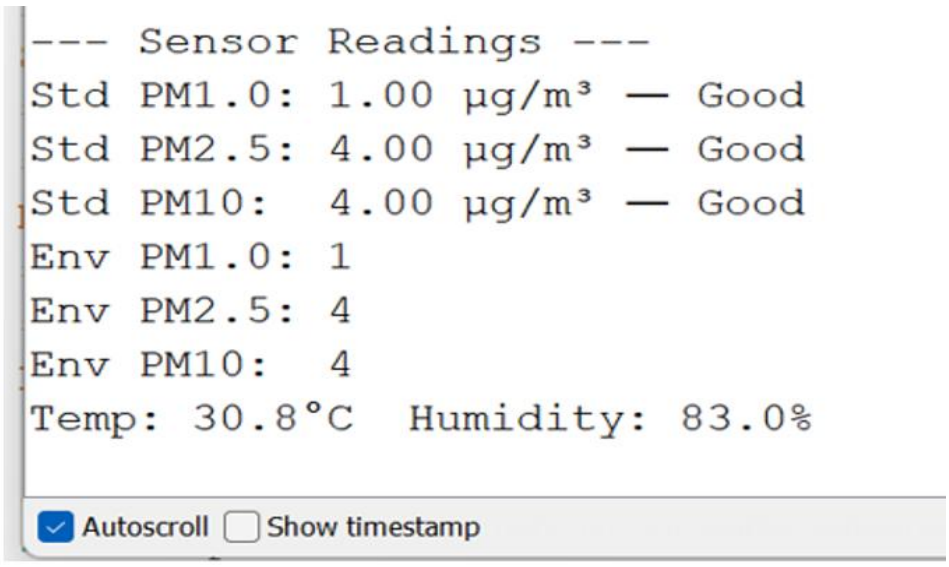


Figure 16. PM readings (baseline, no incense)

ISSN No. 2454-6194 | DOI: 10.51584/IJRIAS |Volume XI Issue IV April 2026

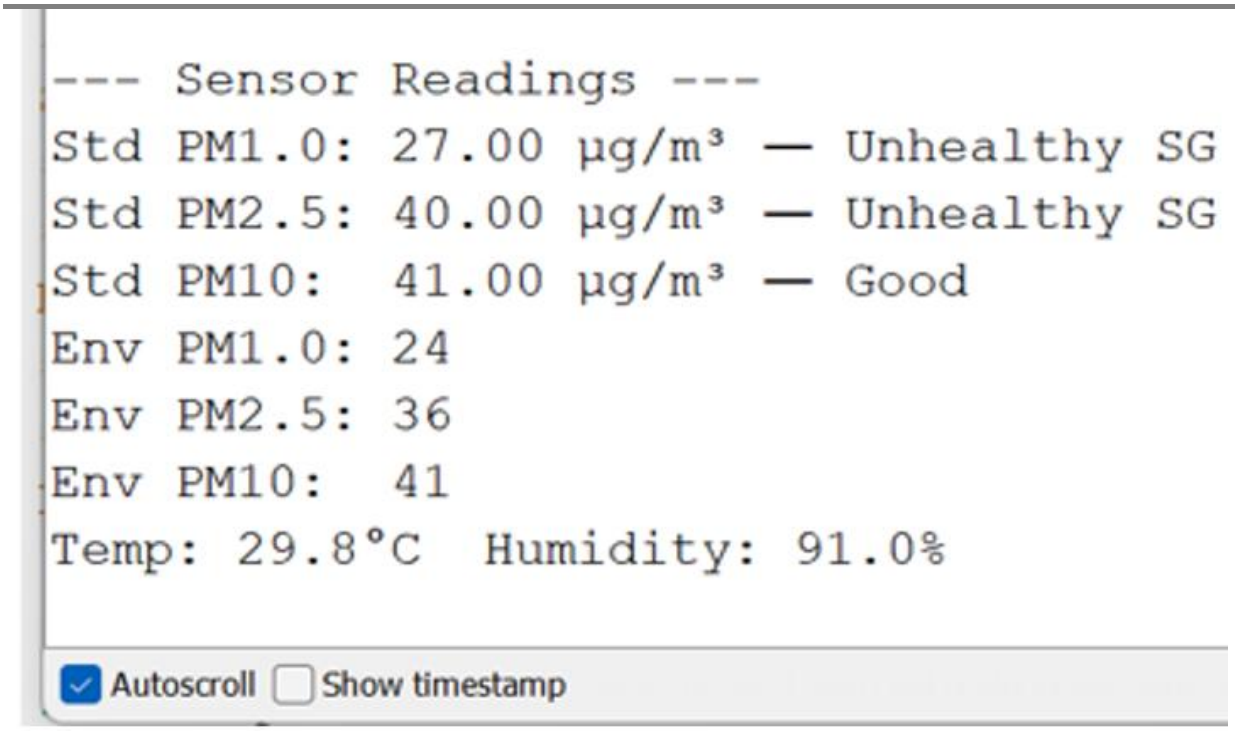


Figure 17. PM response after single incense exposure

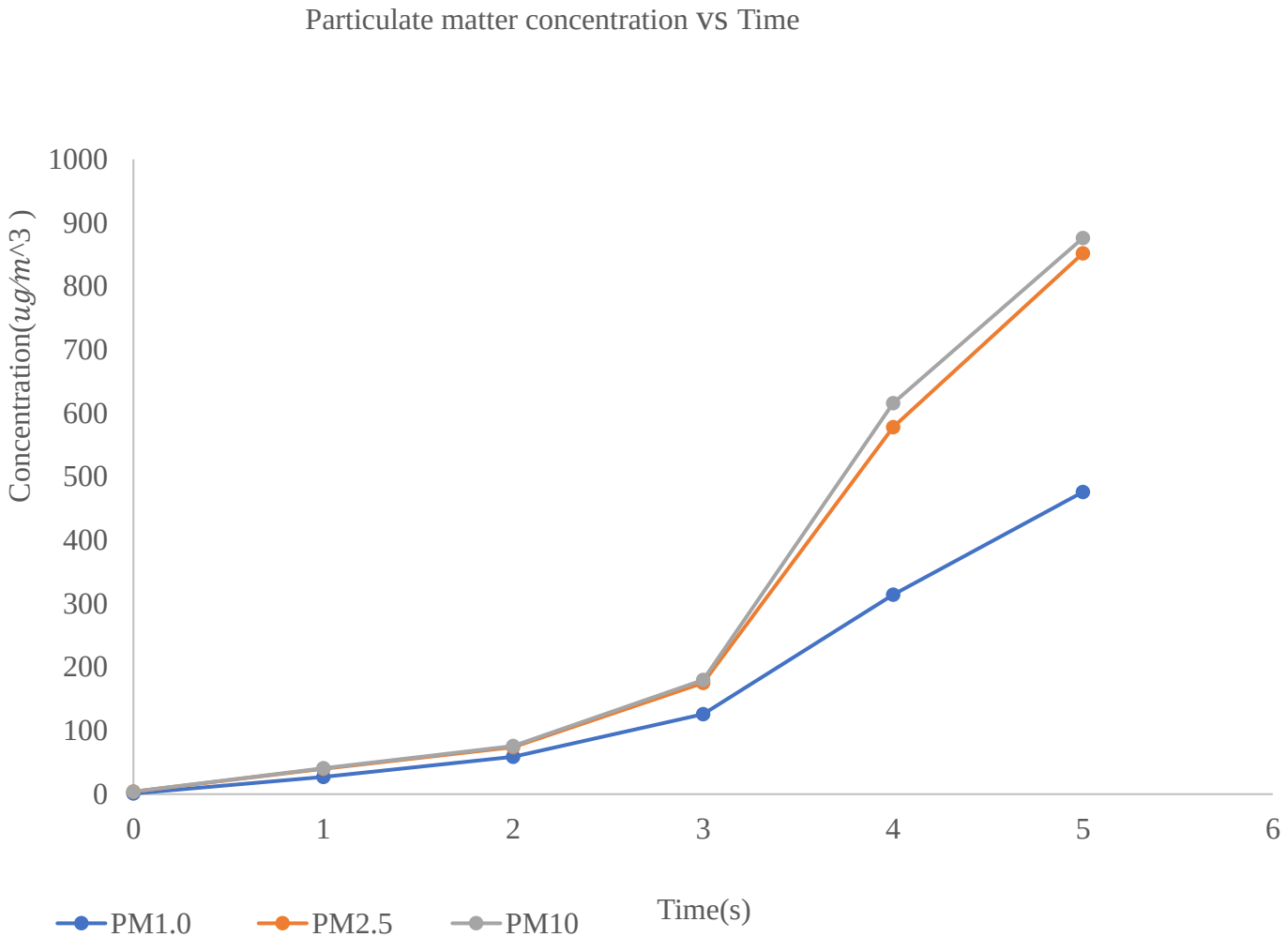


Figure 18. PM concentration vs Time

ISSN No. 2454-6194 | DOI: 10.51584/IJRIAS |Volume XI Issue IV April 2026

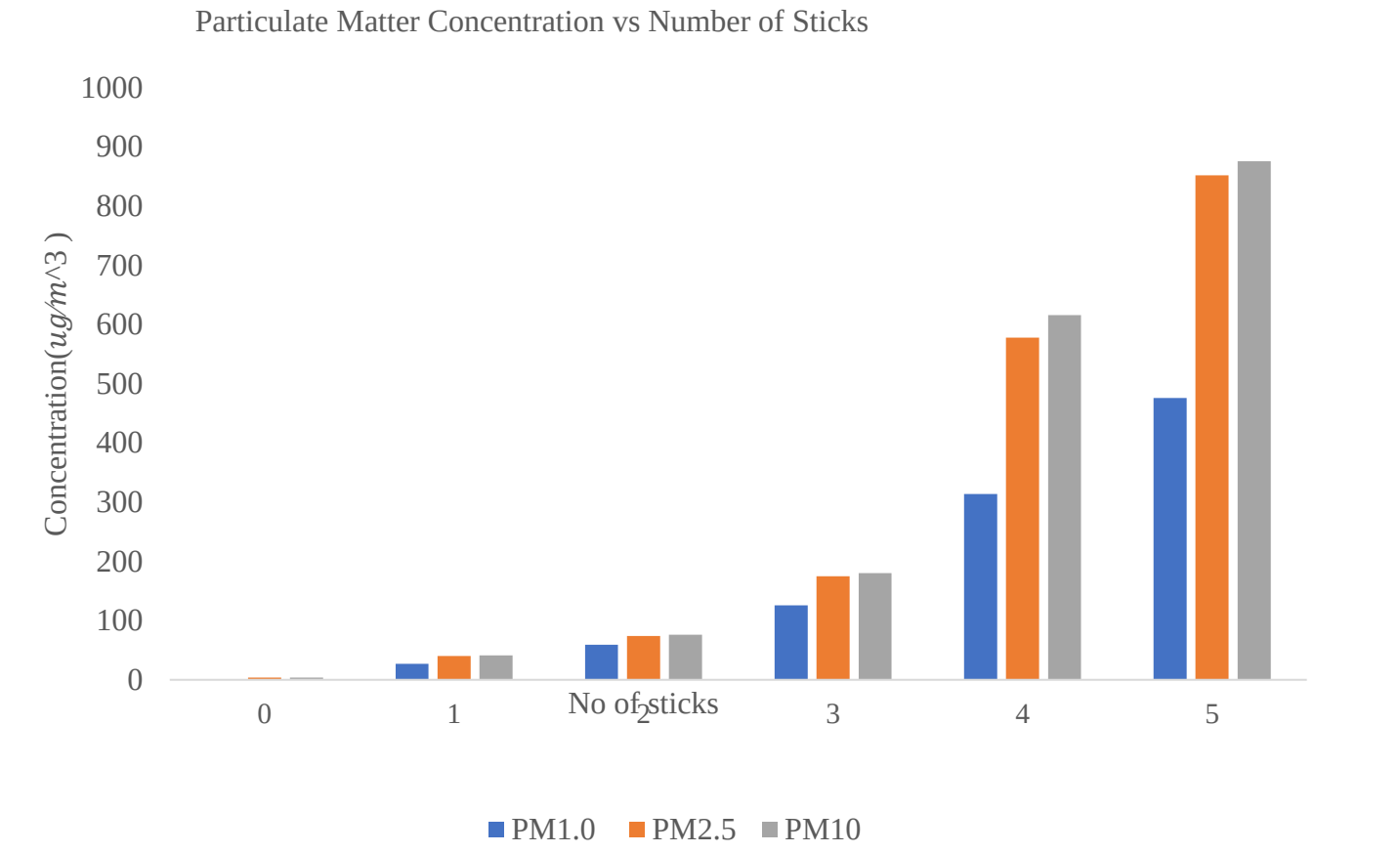


Figure 19. PM concentration vs Number of sticks

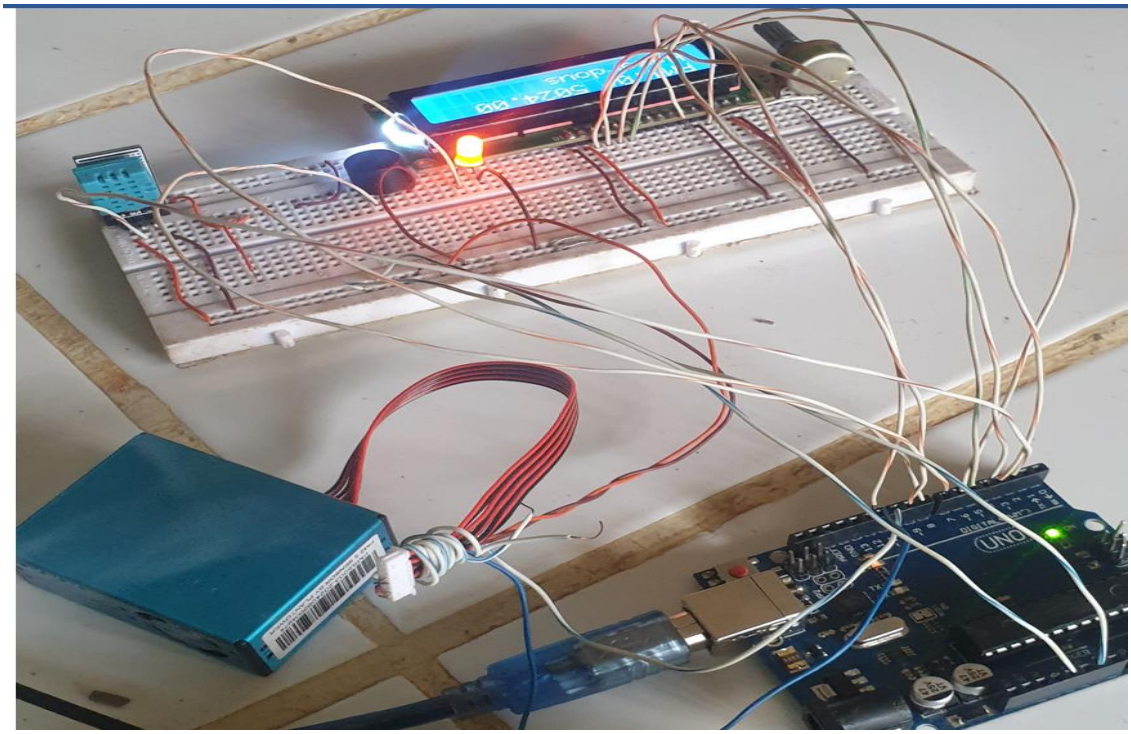

Figure 20. Buzzer and LED alerts under hazardous AQ

## RESULTS AND DISCUSSIONS

In this section, the results of the research are explained, followed by comprehensive discussions. Results are presented in figures, graphs, and tables to facilitate easy understanding. The discussion is structured into sub-sections.

**Particulate Matter Trends**

The experimental results demonstrated a steep rise in particulate matter concentrations ( $PM_{1.0}$ , $PM_{2.5}$ and $PM_{10}$ ) during incense stick exposure. For example, $PM_{2.5}$ levels increased from 4 µg/m³ to 862 µg/m³ within 10 seconds. Baseline values at time zero confirmed clean air conditions, while subsequent data points showed a direct correlation between exposure time and PM accumulation. This trend was consistent across repeated tests (Figure 18).

**Effect of Pollutant Sources**

When the number of incense sticks increased from 0 to 5, PM levels rose exponentially, $PM_{10}$ values, for instance, increased sharply from 4 µg/m³ to 876 µg/m³, these results align with previous findings (Göös et al., 2022). which reported that indoor combustion sources such as incense and cooking contribute significantly to indoor pollution (Table 6 and Figure 19).

**System Responsiveness and Alerts**

The system's LED and buzzer activated during "Unhealthy," "Very Unhealthy," and "Hazardous" AQI conditions, providing real-time alerts (Figure 20), this feature enables immediate corrective actions such as ventilation, reducing exposure risks.

**Sensor Reliability and Cost-effectiveness**

The sensors demonstrated consistent and repeatable responses, with quick return to baseline after exposure. Using low-cost particulate sensors (PMS5003/SDS011) and an environmental sensor (DHT11), the system proved to be a reliable and affordable solution for household and institutional use. Similar approaches have been recommended in recent studies (Gupta & Eden, 2022).

## CONCLUSION

The developed air quality monitoring system successfully detected and responded to varying levels of particulate matter ( $PM_{1.0}$ , $PM_{2.5}$ and $PM_{10}$ ), the correlation between pollutant concentration, exposure time, and pollutant source was confirmed, demonstrating reliable dynamic response and sensitivity. The real-time alert mechanism enhanced its practical use, warning users when indoor air reached unhealthy levels. As expected from the introduction, the results demonstrated compatibility between the proposed system's objectives and its achieved outcomes. Furthermore, this study highlights the potential for future research to extend the system's capabilities, such as integrating wireless data transmission, IoT-based logging, and broader pollutant detection. These developments could further improve accessibility and adoption in resource-limited regions.

## ACKNOWLEDGEMENTS

The authors would like to acknowledge Umaru Ali Shinkafi Polytechnic, Sokoto, and Usmanu Danfodiyo University, Sokoto, for providing technical guidance and support during this research.

## REFERENCES

1. Alfano, B., Barretta, L., Del Giudice, A., De Vito, S., Di Francia, G., Esposito, E., et al. (2020). Sensors, 20(23), 6819.
2. Anuar, N. A., Jalaludin, N. A., & Sadun, A. S. (2024). Progress in Engineering Application and Technology, 5(1), 259–266.
3. Barbon, G., Margolis, M., Palumbo, F., Raimondi, F., & Weldin, N. (2016). Computer Communications, 89, 128–140.
4. Benko, D., Molnar, A., & Imre, K. (2009). Időjárás, 113, 157–175.
5. Concas, F., Mineraud, J., Lagerspetz, E., Varjonen, S., Liu, X., Puolamäki, K., et al. (2021). Low-cost outdoor air quality monitoring and sensor calibration: A survey and critical analysis. ACM Transactions on Sensor Networks, 17(2), 1–44.

6. Dewage, P. M. H. (2024). Physical sensing of airborne particulates using complementary in-situ and remote sensing approaches (Doctoral dissertation). University of Texas at Dallas.
7. Elabd, E., Hamouda, H. M., Ali, M. M., Hamid, A., & Fouad, Y. (2026). Scientific Reports.
8. Flohr, J., Dritz, S., Tokach, M. D., Woodworth, J., DeRouchey, J. M., & Goodband, R. D. (2018). Animal, 12(5), 1022–1029.
9. Göös, H., Kinnunen, M., Salokas, K., Tan, Z., Liu, X., Yadav, L., et al. (2022). Nature Communications, 13(1), 766.
10. Gupta, M., & Eden, G. (2022). The human-air interface: Responding to poor air quality through lived experience and digital information. In Proceedings of the 2022 ACM Designing Interactive Systems Conference.
11. He, M., Kuerbanjiang, N., & Dhaniyala, S. (2020). Performance characteristics of the low-cost Plantower PMS optical sensor. Aerosol Science and Technology, 54(2), 232–241.
12. Huang, Y., Du, W., Chen, Y., Shen, G., Su, S., Lin, N., et al. (2017). Environmental Pollution, 231, 635–643.
13. Ji, X., Le Bihan, O., Ramalho, O., Mandin, C., D'Anna, B., Martinon, L., et al. (2010). Indoor Air, 20(2), 147–158.
14. Johari, S., Goel, I., & Mandal, A. (2017). Health effects of ultrafine particles (PM1.0): A review. Materials Science, 3, 1–10.
15. Kloppenborg, A., Frederickson, L. B., Nielsen, R. Ø., Sabel, C. E., Skallgaard, T., Löndahl, J., et al. (2026). Sensors, 26(1), 280.
16. Kumar, P., Skouloudis, A. N., Bell, M., Viana, M., Carotta, M. C., Biskos, G., & Morawska, L. (2016). Science of the Total Environment, 560, 150–159.
17. Ma, N., Kang, Y., Gan, W., & Zhou, J. (2025). Current Pollution Reports, 11(1), 45.
18. Maag, C., Zhou, Z., & Thiele, L. (2018). IEEE Internet of Things Journal, 5(6), 4857–4870.
19. Mahajan, S., & Helbing, D. (2025). npj Climate and Atmospheric Science, 8(1), 257.
20. Mukherjee, A., & Agrawal, M. (2017). Reviews of Environmental Contamination and Toxicology, 244, 5–51.
21. Perez, B. G. (2025). Empowering Navajo communities through citizen science (Doctoral dissertation). Northern Arizona University.
22. Sayahi, T., Butterfield, A., & Kelly, K. E. (2019). Environmental Pollution, 245, 932–940.
23. Singer, B. C., & Delp, W. W. (2018). Indoor Air, 28(4), 624–639.
24. Thorpe, A., & Harrison, R. M. (2008). Science of the Total Environment, 400(1–3), 270–282.
25. Zhao, Y., Cheng, Z., Lu, Y., Chang, X., Chan, C., Bai, Y., et al. (2017). Environmental Technology Reviews, 6(1), 174–185.
26. Zheng, T., Bergin, M. H., Johnson, K. K., Tripathi, S. N., Shirodkar, S., Landis, M. S., et al. (2018). Atmospheric Measurement Techniques, 11(8), 4823–4846.
27. Zuo, Y., Lai, C., & Iyer, K. L. V. (2023). IEEE Transactions on Power Electronics, 38(9), 11352–11367.